Chinese Physics Letters **42**, 066301 (2025) **Express Letter**

Unprecedented Superionicity of Ultra-Low Barrier in $A_{0.5}CoO_2$ (A = Li, Zn)

Xuechen Wang[1], Yaxin Gao[2], and Menghao Wu[1*]

[1]*School of Physics and School of Chemistry, Huazhong University of Science and Technology, Wuhan 430074, China*
[2]*School of Physics and Mechanical Electrical & Engineering, Hubei University of Education, Wuhan 430205, China*

(Received 16 March 2025; accepted manuscript online 6 May 2025)

The ion conductivity of a solid-state ion conductor generally increases exponentially upon reduction in ion migration barrier. For prevalent cathode material $LiCoO_2$, the room-temperature ion conductivity and migration barrier are respectively around 10^{-4} S/cm and 0.3 eV. In this Letter, through first-principles calculations we predict the existence of 1D superionicity as the Li ions in O2 $LiCoO_2$ are transformed into $Zn_{0.5}CoO_2$ or $Li_{0.5}CoO_2$ via cation-exchange reaction or deintercalation. The ion migration barriers (0.01–0.02 eV) even lower than room-temperature $\sim k_BT$ are reduced by more than an order of magnitude compared with $LiCoO_2$, which are facilitated by facile transition of mobile ions between two coordination configurations. The room-temperature ion conductivity is estimated to be over 50 S/cm, enhanced by 2–3 orders of magnitude compared with the current highest reported value. Such unprecedented superionicity may also exist in other similar layered ion conductors, which may lead to technical advances and exotic effects such as ultrafast ion batteries and quantized ferroelectricity.

DOI: 10.1088/0256-307X/42/6/066301 CSTR: 32039.14.0256-307X.42.6.066301

Solid-state ion conductors exhibiting fast ion transport have been widely used in energy storage devices like batteries.[1–8] In particular, lithium-ion batteries have emerged as an essential component of modern portable power sources. $LiCoO_2$ is one of the most extensively studied cathode materials due to its high energy density and long cycling stability,[9] where the layered structure is formed by Co^{3+}-based edge-sharing CoO_6 octahedrons separated by lithium layers, facilitating the intercalation/deintercalation of Li ions. However, its low room-temperature ion conductivity ($\sim 10^{-4}$ S/cm)[10] due to high migration barrier ($\sim$0.3–0.4 eV)[11–13] would cause not only a sluggish transport of Li ions, but also a significant polarization at the cathode-electrolyte interface. The ion conductivity is proportional to $\exp(-\frac{\Delta}{k_BT})$, which can be significantly enhanced even when the barrier Δ is only slightly reduced. For example, the room-temperature ion conductivity and migration barrier for $LiNbOCl_4$ have been respectively estimated to be 10.4 mS/cm and 0.205 eV,[14] which are 24 mS/cm and 0.155 eV for $Li_{5.3}PS_{4.3}ClBr_{0.7}$ with disorder among Cl^-, Br^- and S^{2-} sites.[15] In 2023, Ryoji Kanno *et al.* synthesized $Li_{9.54}[Si_{1-\delta}M_\delta]_{1.74}P_{1.44}S_{11.1}Br_{0.3}O_{0.6}$ (M = Ge, Sn) with a high room-temperature conductivity of 32 mS/cm and low migration barrier of 0.09 eV, surpassing all previously reported values for inorganic Li-ion conductors.[16] However, even such a low barrier still corresponds to k_BT of a high temperature over 1000 K, surpassing the melting points of many solid-state ion conductors. If the barrier can be reduced below $\sim k_BT$, ions can move as quasi-free particles and the potential wells provide scattering instead of localization, which may give rise to various exotic effects described in the lattice gas model.[17]

Additionally, some solid-state ion conductors with ion vacancies may exhibit unconventional ferroelectricity with quantized polarizations.[18] It has also been proposed that such quantized ferroelectricity may even emerge in monovalent ion conductors with non-ferroelectric crystal lattices if their mobile monovalent cations are substituted by multivalent cations (e.g., Mg^{2+}, Al^{3+})[19] via cation-exchange reaction, based on previous experimental reports on topotactic reaction with an aliovalent cation between trigonal layers of ion conductors.[20,21] However, the experimental realization of such quantized ferroelectricity is also hindered by the high migration barriers of those ion conductors (e.g., 0.31 eV per Na ion for Na_4SnS_4,[18] and 0.29 eV per Mg ion for $Mg_{0.5}CrS_2$,[19] much higher than the switching barrier of $BaTiO_3$ around 0.1 eV). In this Letter, we predict by *ab initio* calculations that when the Li ions in O2 $LiCoO_2$ are substituted by half the number of divalent Zn^{2+} by cation-exchange reaction, or half of them are deintercalated, arrays of 1D ion conduction channels with ultra-low migration barriers (0.01–0.02 eV) will be formed, giving rise to unprecedented room-temperature ion conductivity over 50 S/cm. The ultralow migration barrier can be attributed to the existence of two interconvertible states with different coordinate configurations that are almost degenerate in energy, making the intercalated ions behave like 1D liquids at ambient conditions.

Our theoretical calculations are performed based on density functional theory (DFT) methods implemented in the Vienna Ab Initio Simulation Package (VASP) software.[22,23] The generalized gradient approximation (GGA) in the form of Perdew-Burke-Ernzerhof functional (PBE)[24] and the projector augmented wave (PAW)[25] method are applied to describe the exchange-correlation

*Corresponding author. Email: wmh1987@hust.edu.cn
© 2025 Chinese Physical Society and IOP Publishing Ltd. All rights, including for text and data mining, AI training, and similar technologies, are reserved.

and the core electrons, respectively. PBE + U method with an effective U value (U_{eff}) of 4.9 eV [26] is used to account for strong correlation. The kinetic energy cutoff was set at 500 eV, and the Brillouin zone was sampled by $7 \times 5 \times 3$ K points for O2-state and $5 \times 7 \times 5$ K points for O3-state using the Monkhorst–Pack scheme. [27] The convergence threshold for self-consistent-field iteration was set to 10^{-6} eV and all structures are fully optimized until the forces are smaller than 0.01 eV/Å. The Berry phase method was employed to evaluate crystalline polarizations, and the ion migration pathways were obtained by using the solid-state nudged elastic band (SSNEB) [28] method.

The experimentally verified O3 and O2 phase $LiCoO_2$ respectively with parallel and antiparallel CoO_2 layers are displayed in Fig. 1, where the Li ions are intercalated into the interstitial octahedral sites. [29–32] As the Li ions are substituted by half the number of Zn ions, the CoO_2 layers in O2 phase $ZnCo_2O_4$ become buckled in the ground state (see the comparison in energy between different configurations in Fig. S1), which are still planar in O3 phase. Two configurations may form in O2 $ZnCo_2O_4$, where each Zn ion can either bond with 6 O atoms in a ZnO_6 octahedron (denoted as Oct-state), or 4 O atoms in a ZnO_4 tetrahedron (denoted as Tet-state, only 2 meV/f.u. higher in energy compared with Oct-state). The bonding configurations of Zn ions in two phases are shown in Fig. 1(b), where the Zn-O bond lengths in Tet-state range from 1.998 to 2.018 Å ($d_{\text{Zn-O1}} = d_{\text{Zn-O3}} = 1.998$ Å, $d_{\text{Zn-O2}} = d_{\text{Zn-O4}} = 2.018$ Å), mostly shorter compared with Oct-state ($d_{\text{Zn-O1}} = d_{\text{Zn-O2}} = 2.226$ Å, $d_{\text{Zn-O5}} = d_{\text{Zn-O6}} = 2.195$ Å, $d_{\text{Zn-O3}} = 2.015$ Å, $d_{\text{Zn-O4}} = 2.043$ Å), and the differences between those bond lengths reveal the distortions of octahedrons and tetrahedrons.

As shown in Fig. 2 where adjacent in-plane O atoms of each layer are linked, each Zn cation in $LiCoO_2$ is located between two antiparallel oxygen triangles of adjacent layers respectively marked in red and blue, with overlapping centers from the overview. As Li ions are substituted by half the number of Zn ions, the deviations between the centers of two triangles upon slightly interlayer sliding make them staggered in the Oct-phase $Zn_{0.5}CoO_2$, accompanied by the distortions of ZnO_6 octahedrons. According to our NEB calculations, the transition barrier between Oct and Tet-phase upon displacements of Zn ions (accompanied by slightly interlayer sliding of 0.65 Å) is only around 20 meV per Zn ion.

It is noteworthy that when half of Li ions in O2 $LiCoO_2$ are deintercalated, similar Oct and Tet-phase for $LiCo_2O_4$ may emerge with a small energy difference around 5 meV/f.u. between them, and their transition barrier of 13 meV/f.u. is even lower, although it is metallic, unlike insulating $ZnCo_2O_4$ with a bandgap of 1.27 eV. Similar low migration barrier may also exist in some other layered ion conductors like $ZnNi_2O_4$ (see the estimated value around 33 meV in Fig. S2). Compared with the ground state with pyrochlore lattices, such layered structures are respectively 64 and 36 meV/f.u. higher in energy for $ZnCo_2O_4$ and $ZnNi_2O_4$, so their stable formations via cation-exchange reaction from O2 $LiCoO_2$ should be still possible. According to our *ab initio* molecular dynamic (AIMD) simulations in the canonical ensemble at a controlled temperature of 600 K (Fig. S3), the robust integrity of layered structure suggests good thermal stability.

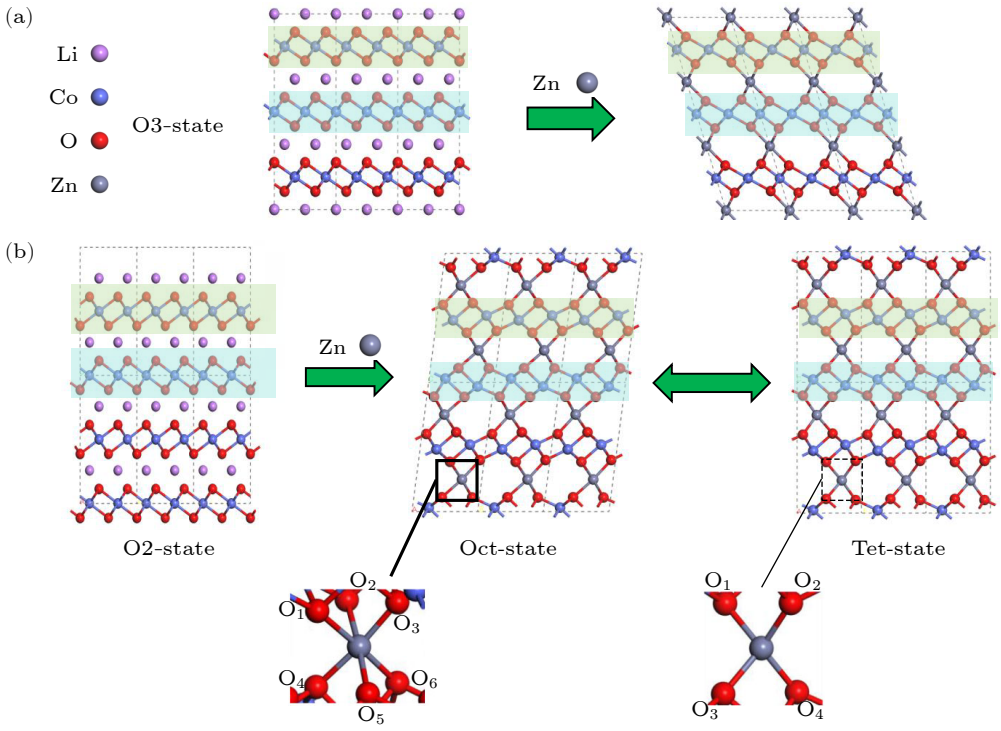

Fig. 1. (a) Transformation from O3 state $LiCoO_2$ to $ZnCo_2O_4$ upon cation-exchange reaction. (b) Transformation from O2 state $LiCoO_2$ to Oct and Tet state $ZnCo_2O_4$, respectively with distorted ZnO_6 octahedrons and ZnO_4 tetrahedrons.

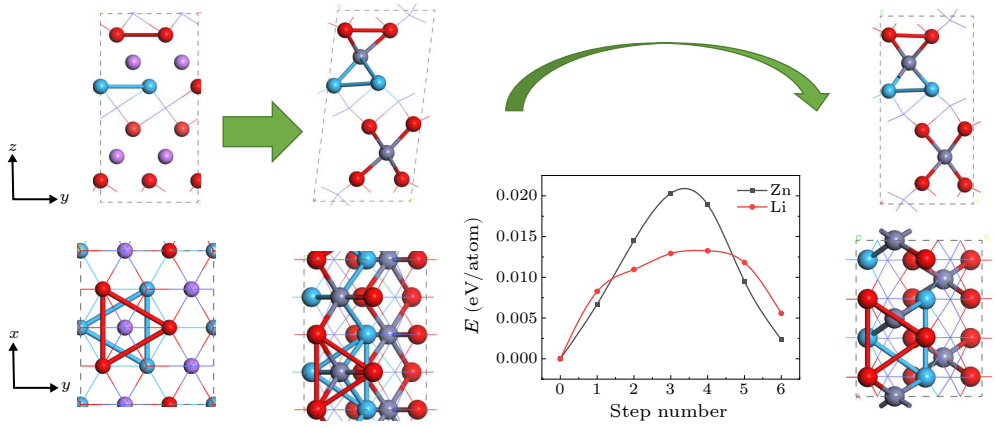

Fig. 2. The side view and overview of O2 $LiCoO_2$, Oct and Tet state of $ZnCo_2O_4$, and Oct-Tet phase transition pathways for $ZnCo_2O_4$ and $LiCo_2O_4$, where the upper and lower oxygen triangles are marked in red and blue, respectively.

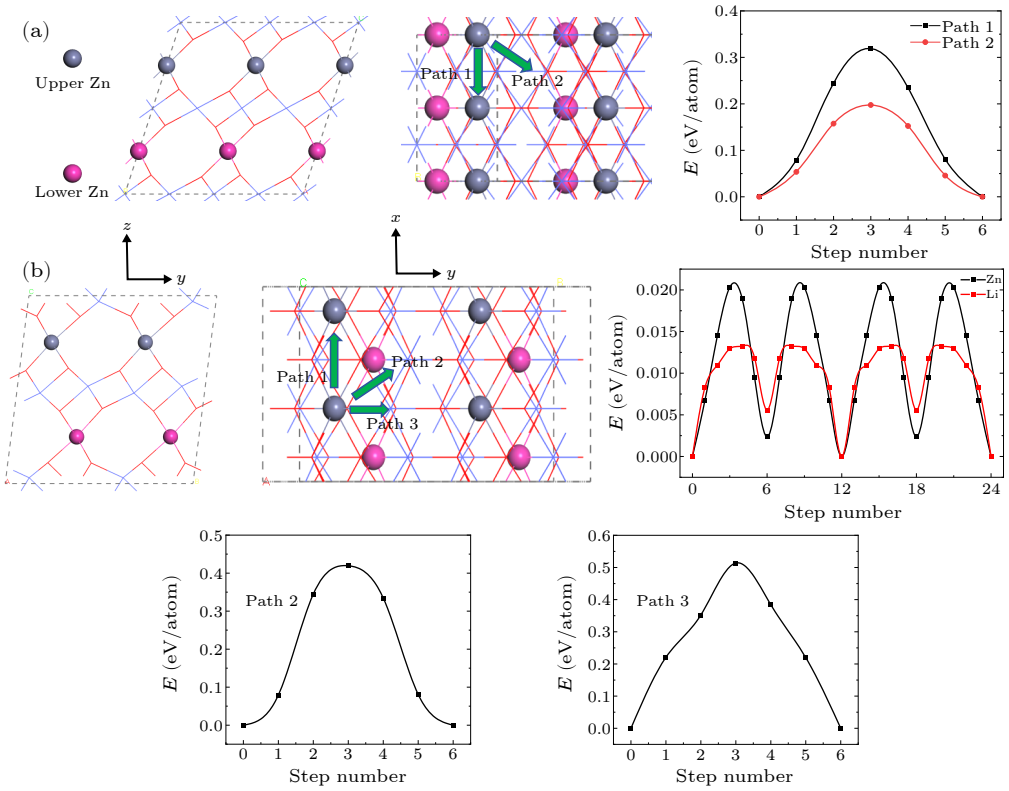

Fig. 3. (a) The sideview (left) and overview (right) structure of O3-$ZnCo_2O_4$ and two ion migration pathways. (b) The sideview (left) and overview (right) structure of O2-$ZnCo_2O_4$ and three ion migration pathways, where the migration along path 1 also gives ultralow barrier for O2-$LiCo_2O_4$.

The in-plane migration barrier of Li ions in O3 $LiCoO_2$ is typically ∼0.3–0.4 eV according to previous studies,[11,12] which is reduced to ∼0.2–0.3 eV per Zn ion upon cation-exchange reaction, as shown in Fig. 3(a) and Fig. S4. In the anti-parallel stacking configuration, the migration of Zn ions along the $-x$ direction can be greatly facilitated by the low barrier of Oct-Tet phase transition where the Zn ions are displaced by half lattice constant $|\boldsymbol{a}|/2$, while the structural configuration is unchanged upon the translation of Zn ions for one lattice constant $|\boldsymbol{a}|$ in the periodic crystal model, so the process of migration for one lattice constant will be equivalent to Oct-Tet-Oct phase transition. As shown in Fig. 3(b), the migration barrier along the conduction channel is just the Oct-Tet phase transition barrier, even lower than $\sim k_{\mathrm{B}}T$ at ambient conditions and more than an order of magnitude lower compared with migration barrier in O3 phase. Meanwhile the migration barriers along other two directions [marked as paths 2 and 3 in Fig. 3(b)] are much higher (all over 0.4 eV). Such anisotropy should clarify the formations of confined 1D

ion liquids in Fig. S3, where the displacements of Zn ions along the $-y$ direction at elevated temperature are negligible compared with the $-x$ direction. Although a number of specialized electronic conduction and ion transport properties can be attributed to the ligand field environment in previous studies,[33–36] herein the bandstructures in Fig. S5 reveal that the bandstructures for Oct and Tet states of O2 are almost the same, which are even more insulating compared with O3 state, suggesting that the high ion conductivities should be attributed to the facile coordination translation of low barriers instead of ligand field environment.

A coarse estimation of ion conductivity ($\delta_{\rm ion}$)[37] can be formulated as

$$\delta_{\rm ion} = \Big(\frac{\gamma c \nu Z^2 {\rm e}^2 a_0^2}{k_{\rm B}T}\Big) \exp\Big(-\frac{\Delta G_{\rm m}}{k_{\rm B}T}\Big),$$

where $Z = 2$ is the charge number of Zn ion, $a_0 = 3.03 \times 10^{-8}$ cm and $\Delta G_{\rm m} = 0.02$ eV are respectively the transfer distance and migration barrier of each Zn ion. $c = 0.012 \times 10^{24}\,{\rm cm}^{-3}$ is its ion density, $\nu = 10^{13}\,{\rm s}^{-1}$ is the frequency and $\gamma = 1$ represents the 1D Zn ion conduction channel. Given the parameters above, $\delta_{\rm ion}$ is estimated to be 55.6 S/cm for $ZnCo_2O_4$. Similarly, the Li ion conductivity in O2 $LiCo_2O_4$ estimated to be 27.3 S/cm is not only 5 orders of magnitude larger than δ in O3 $LiCoO_2$[10] (10^{-4} S/cm), but also much higher than all superionic crystals currently known, like lithium argyrodites[38] (~10 mS/cm), α-$RbAg_4I_5$[39] (0.3 S/cm) and α-KAg_4I_5(0.221 S/cm).[40] However, such ultrahigh conductivity is highly anisotropic since the migration barrier is much higher along two other directions, where the coordination phase transition is not involved.

We use the following equation for a rough estimation of the specific capacity of $ZnCo_2O_4$ as a cathode material:

$$C = \frac{nZ{\rm F}}{3.6m},$$

where $n = 1$ is the mole number of Zn ion, $Z = 2$ is the charge number of Zn ion, F is the Faraday constant (F = 96485 C·mol^{-1}), and $m = 247.24$ g·mol^{-1} is the mole mass of $ZnCo_2O_4$. Given the parameters above, C is estimated to be 216.44 mAh/g. It is noteworthy that this value is an upper limit since the entire extraction of Zn ions could lead to structural collapse, and it is comparable to the similar upper limit of capacity 274 mAh/g for $LiCoO_2$. The open-circuit voltage (OCV) of $ZnCo_2O_4$ in Fig. 4(a) estimated to be 4.88 V is higher than most Li-ion cathode materials such as $LiCoO_2$ (3.75 V) and $LiFePO_4$ (3.47 V),[11] and the estimated energy density of 1056.3 Wh/kg is also higher ($LiCoO_2$:760/1027.5 Wh/kg in experimental/theoretical reports; $LiFePO_4$: 476/590 Wh/kg in experimental/theoretical reports).[41] With high energy density and ultra-low migration barrier, $ZnCo_2O_4$ could be a promising material for ultra-fast rechargeable ion battery.

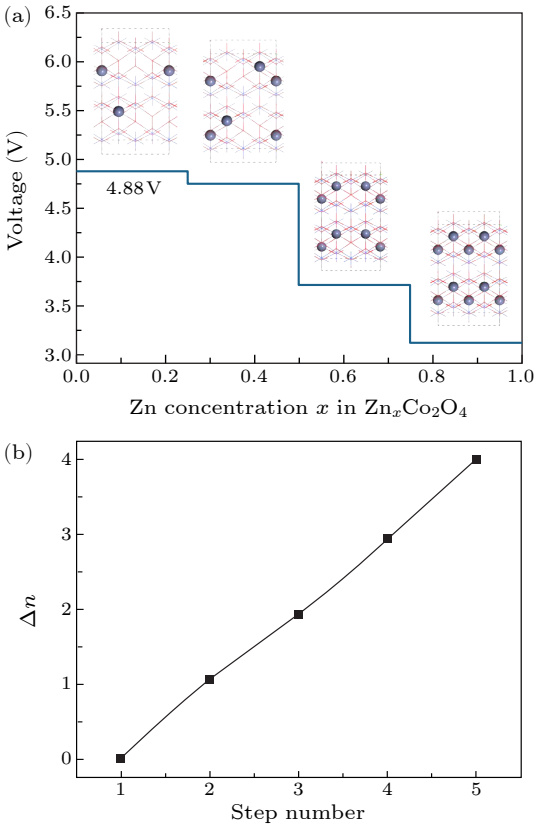

Fig. 4. (a) Calculated open-circuit voltage (OCV) as a function of Zn-ion concentration x in $Zn_xCo_2O_4$. (b) The polarization quantum evolution upon the migration of Zn ions along the $-x$ direction for one lattice constant $|\boldsymbol{a}|$, where $\Delta n = \Omega \Delta P/{\rm e}|\boldsymbol{a}|$.

Finally, the low ion migration barrier of $ZnCo_2O_4$ should facilitate the realization of unconventional ferroelectricity with quantized polarization, considering the unattainable voltage required for switching due to the high barriers over 0.3 eV in previous predicted systems.[18,19] Upon migration of Zn ions for one lattice constant along the $-x$ direction corresponding to 1 ion vacancy at each channel, the change of polarization quanta $\Delta n = 4 = \Omega \Delta P/{\rm e}|\boldsymbol{a}|$ in Fig. 4(b), and the switchable polarization $P = \Delta P/2 = 2{\rm e}|\boldsymbol{a}|/\Omega = 63.6\,\mu{\rm C/cm}^2$(where Ω is the unitcell volume and $|\boldsymbol{a}|$ is the lattice constant), already two times larger compared with $BaTiO_3$. In a $ZnCo_2O_4$ crystal with size ~1 μm and a density of only 1 vacancy per 100 Zn ions, the migration distance in each channel will be orders of magnitude larger, giving rise to an immense ferroelectric polarization around ~1000 μC/cm^2, with barriers comparable to those of current ferroelectrics.[42–44]

In summary, we predict the existence of superionicity in antiparallel stacking $ZnCo_2O_4$ and $LiCo_2O_4$ based on O2 $LiCoO_2$. The ultralow transition barriers (0.01–0.02 eV) between Oct and Tet states are also the ion migration barrier along the 1D conduction channels, leading to the highest solid-state ion conductivity known to date. Similar superionicity may also exist in some other layered ion conductors like $ZnNi_2O_4$. Considering the technical advances and various exotic effects[17] that may be brought by such elusive superionicity with barriers below room-temperature ~$k_{\rm B}T$, our prediction should deserve

further experimental efforts. We note that phase alteration from O3 to O2 phase for $LiCoO_2$ has been experimentally realized,[45] and if single crystal O2 $ZnCo_2O_4$ and $LiCo_2O_4$ can be synthesized upon cation-exchange reaction or deintercalation on O2 phase $LiCoO_2$, the unprecedented high ion conductivity should be detectable. Such anisotropic ion conduction may also be explored for new functional devices, and it has also been shown that in-plane anisotropic ion migration may couple with gate tunability in 2D semiconductors, which may lead to ion-electron co-modulations in three-terminal-based charge transport.[46]

Acknowledgements. This work is supported by the National Natural Science Foundation of China (Grant No. 22073034).

References

[1] Rickert H 1978 *Angew. Chem. Int. Ed. Engl.* **17** 37
[2] Sebti E, Evans H A, Chen H, Richardson P M, White K M, Giovine R, Koirala K P, Xu Y, Gonzalez-Correa E, Wang C, Brown C M, Cheetham A K, Canepa P, and Clément R J 2022 *J. Am. Chem. Soc.* **144** 5795
[3] Zhang Z, Roy P N, Li H, Avdeev M, and Nazar L F 2019 *J. Am. Chem. Soc* **141** 19360
[4] Li M, Pietrowski M J, De Souza R A, Zhang H, Reaney I M, Cook S N, Kilner J A, and Sinclair D C 2014 *Nat. Mater.* **13** 31
[5] Peng J, Liu Y, Pan Y, Wu J, Su Y, Guo Y, Wu X, Wu C, and Xie Y 2020 *J. Am. Chem. Soc.* **142** 18645
[6] Nishijima M, Ootani T, Kamimura Y, Sueki T, Esaki S, Murai S, Fujita K, Tanaka K, Ohira K, Koyama Y, and Tanaka I 2014 *Nat. Commun.* **5** 4553
[7] Jun K, Sun Y, Xiao Y, Zeng Y, Kim R, Kim H, Miara L J, Im D, Wang Y, and Ceder G 2022 *Nat. Mater.* **21** 924
[8] Jun K, Chen Y, Wei G, Yang X, and Ceder G 2024 *Nat. Rev. Mater.* **9** 887
[9] Lyu Y, Wu X, Wang K, Feng Z, Cheng T, Liu Y, Wang M, Chen R, Xu L, Zhou J, Lu Y, and Guo B 2021 *Adv. Energy. Mater.* **11** 2000982
[10] Slima I B, Karoui K, and Rhaiem A B 2023 *Ionics.* **29** 1731
[11] Zhang T, Li D, Tao Z, and Chen J 2013 *Prog. Nat. Sci.* **23** 256
[12] Ning F, Li S, Xu B, and Ouyang C 2014 *Solid. State. Ionics.* **263** 46
[13] Aydinol M K, Kohan A F, Ceder G, Cho K, and Joannopoulos J 1997 *Phys. Rev. B* **56** 1354
[14] Tanaka Y, Ueno K, Mizuno K, Takeuchi K, Asano T, and Sakai A 2023 *Angew. Chem. Int. Edit.* **62** e202217581
[15] Patel S V, Banerjee S, Liu H, Wang P, Chien P H, Feng X, Liu J, Ong S P, and Hu Y Y 2021 *Chem. Mater.* **33** 1435
[16] Li Y, Song S, Kim H, Nomoto K, Kim H, Sun X, Hori S, Suzuki K, Matsui N, Hirayama M, Mizoguchi T, Saito T, Kamiyama T, and Kanno R 2023 *Science* **381** 50
[17] Dieterich W, Fulde P, and Peschel I 1980 *Adv. Phys.* **29** 527
[18] Wang X, Ren Y, and Wu M 2022 *J. Phys. Chem. Lett.* **13** 9552
[19] Wang X and Wu M 2024 *Mater. Horiz.* **11** 3885
[20] Heubner C, Lein T, Schneider M, and Michaelis A 2020 *J. Mater. Chem. A* **8** 16854
[21] Miura A, Takei T, and Kumada N 2013 *J. Solid. State. Chem.* **197** 471
[22] Kresse G and Furthmüller J 1996 *Comp. Mater. Sci.* **6** 15
[23] Kresse G and Furthmüller J 1996 *Phys. Rev. B* **54** 11169
[24] Perdew J P, Ruzsinszky A, Csonka G I, Vydrov O A, Scuseria G E, Constantin L A, Zhou X, and Burke K 2008 *Phys. Rev. lett.* **100** 136406
[25] Blöchl P E 1994 *Phys. Rev. B* **50** 17953
[26] Zhou F, Cococcioni M, Marianetti C A, Morgan D, and Ceder G 2004 *Phys. Rev. B* **70** 235121
[27] Monkhorst H J and Pack J D 1976 *Phys. Rev. B* **13** 5188
[28] Henkelman G, Uberuaga B P, and Jónsson H 2000 *J. Chem. Phys.* **113** 9901
[29] Li S, Sun Y, Gao A, Zhang Q, Lu X, and Lu X 2022 *Proc. Natl. Acad. Sci.* **119** e2120060119
[30] Yabuuchi N, Kawamoto Y, Hara R, Ishigaki T, Hoshikawa A, Yonemura M, Kamiyama T, and Komaba S 2013 *Inorg. Chem.* **52** 9131
[31] Carlier D, Van der Ven A, Delmas C, and Ceder G 2003 *Chem. Mater.* **15** 2651
[32] Carlier D, Saadoune I, Croguennec L, Ménétrier M, Suard E, and Delmas C 2001 *Solid. State. Ionics.* **144** 263
[33] Wang Z, Wang D, Zou Z, Song T, Ni D, Li Z, Shao X, Yin W, Wang Y, Luo W, Wu M, Avdeev M, Xu B, Shi S, Ouyang C, and Chen L 2020 *Natl. Sci. Rev.* **7** 1768
[34] Wang D, Jiao Y, Shi W, Pu B, Ning F, Yi J, Ren Y, Yu J, Li Y, Wang H, Li B, Li Y, Nan C, Chen L, and Shi S 2023 *Prog. Mater. Sci.* **133** 101055
[35] Yu J, Wang D, Wang G, Cui Y, and Shi S 2023 *Adv. Mater.* **35** 2209210
[36] Wang D, Yu J, Yin X, Shao S, Li Q, Wang Y, Avdeev M, Chen L, and Shi S 2023 *Natl. Sci. Rev.* **10** nwad010
[37] Ohno S, Banik A, Dewald G F, Kraft M A, Krauskopf T, Minafra N, Till P, Weiss M, and Zeier W G 2020 *Prog. Energy.* **2** 022001
[38] Zhou L, Assoud A, Zhang Q, Wu X, and Nazar L F 2019 *J. Am. Chem. Soc.* **141** 19002
[39] Shabanov O M, Kachaev R T, and Kazieva L A 2012 *Tech. Phys.* **57** 1157
[40] Andreeva A V and Despotuli A L 2005 *Ionics.* **11** 152
[41] Yu Q, Tang W, Hu Y, Gao J, Wang M, Liu S, Lai H, Xu L, and Fan C 2021 *Chem. Eng. J.* **415** 128509
[42] Li L and Wu M 2017 *ACS. Nano.* **11** 6382
[43] Wu M and Zeng X C 2016 *Nano. Lett.* **16** 3236
[44] Yang Q, Wu M, and Li J 2018 *J. Phys. Chem. Lett.* **9** 7160
[45] Zan M, Xie H, Jiao S, Jiang K, Wang X, Xiao R, Yu X, Li H, and Huang X 2024 *Small. Sci.* **4** 2400162
[46] Sun Y, Zhang R, Tan J, Zeng S, Li S, Wei Q, Zhang Z Y, Zhao S, Zou X, Liu B, and Cheng H M 2025 *Sci. Adv.* **11** eadr3105